



STRUT-AND-TIE MODELING OF R.C. CONTINUOUS DEEP BEAMS

F.B.A. Beshara¹, I.G. Shaaban² and T.S. Mustafa³

¹ Associate Professor, fouad.beshara@feng.bu.edu.eg

² Professor of Reinforced Concrete Structures, ibrahim.shaaban@feng.bu.edu.eg

³ Assistance Professor, tarek.mohamed@feng.bu.edu.eg

Civil Engineering Department, Faculty of Engineering at Shoubra, Benha University, Egypt

Abstract: A strut-and-tie model (STM) is proposed for the shear carrying capacity of continuous RC deep beams. First, the mathematical formulation is given to fully describe the geometry, derivation of internal forces, evaluation of compressive and tensile stresses, and consideration of concrete tension softening. Second, validation studies for the modified STM are made for number of tested beams from the literature. Finally, a comparative study is presented between the results of proposed STM with the models of ECP code and the ACI code.

Key words: Introduction Continuous deep beams; Strut-and-tie method; Shear strength capacity; Concrete tension softening; Failure mechanism

1. Introduction

The strut-and-tie method can be used for the design of Disturbed regions (D-regions) of structures where the basic assumption of flexure theory, namely plane sections remaining plane before and after bending, does not hold true. Such regions occur near statical discontinuities arising from concentrated forces or reactions and near geometric discontinuities, such as abrupt changes in cross section. The strut-and-tie method of design is based on the assumption that the D-regions in concrete structures can be analyzed and designed using hypothetical pin-jointed trusses consisting of struts and ties inter-connected at nodes. Since continuous deep beams contain significant extents of D-regions and they exhibit a marked truss or tied arch action, the strut-and-tie method offers a rational basis for the analysis and design of such beams. The current paper is a part of a series of a larger research carried out earlier by the authors regarding experimental and theoretical studies for continuous deep beams [1]. The formulation and results for the proposed STM is given herein.

2. Strut-and-Tie Model (STM) of Continuous Deep Beams

The proposed model is an extension to STM; proposed earlier for continuous deep beams [2]. A STM for two-span continuous deep beams with a top point load at each mid-span is given in Fig. (1). It can be idealized as a statically indeterminate truss as shown in Fig. (2). The deep beam under consideration can be assumed to be made up of a primary negative moment truss and a primary positive moment truss as presented in Fig. (2). The location and orientation of the struts and ties are defined by the position of the nodes. The horizontal position of the nodes can be assumed to lie on the line of action of the respective applied loads and the support reactions. For vertical position of nodes, in order to exploit the full load carrying capacity of the beam, it is imperative that nodes A, B and A' lie as close as possible to the bottom face of the beam. Similarly, the nodes C and C' assumed to lie as close as possible to the top face of the beam with providing sufficient concrete cover to the tie reinforcement.

The inclined angle of the diagonal strut θ_s can be obtained by:

$$\tan\theta_s = (h - l_c/2 - l_d/2) / a = (h - c_1 - c_2) / (l_e / 2) \quad (1)$$

Where l_e is the effective span measured between centre-to-centre of supports, h is the beam total depth, a is the shear span measured from centre lines between the load and support bearing plates, l_c and l_d are the respective depths of bottom and top nodal zones as shown in Fig. (3) and were taken as:

$$l_c = 2 c_2 \quad (2)$$

$$l_d = 2 c_1 \quad (3)$$

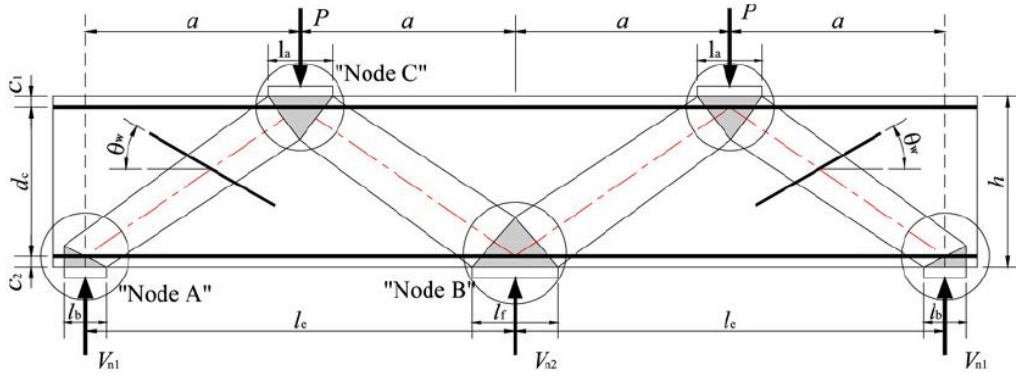


Figure (1) Two-Span Continuous Deep Beam under Two-Point Loading

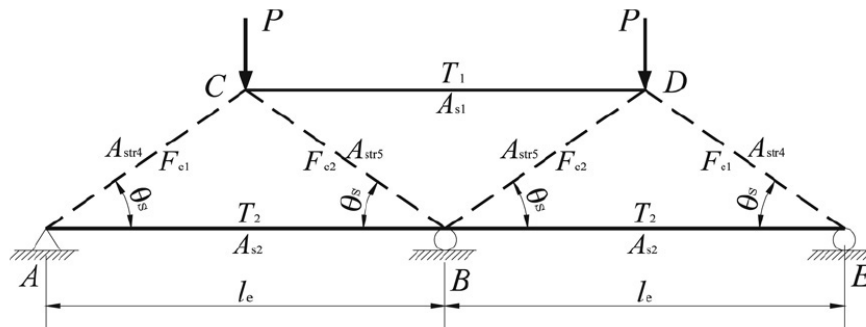


Figure (2) Truss Model for Two-Span Continuous Deep Beam

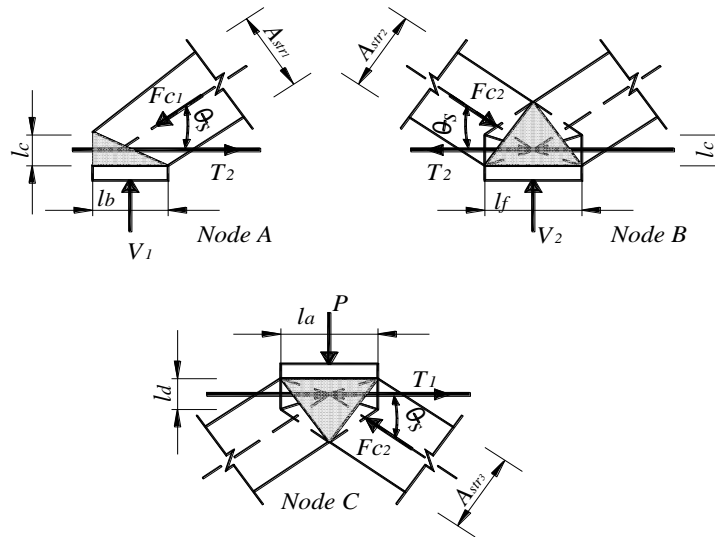


Figure (3) Details of Nodal Zones in Continuous Deep Beams

c_1 and c_2 are the distances from the centroid of the top and bottom longitudinal steel bars to the beam top and beam soffit respectively. The terms A_{str1} , A_{str2} and A_{str3} are assumed to be the cross-sectional areas at the ends of the tapered concrete struts (Fig. (3)), while A_{str4} and A_{str5} represent the average cross-sectional areas of the outer and inner tapered concrete struts, respectively as shown in Fig. (2). They are expressed as follows:

$$A_{str1} = b_w (l_c \cos\theta_s + l_b \sin\theta_s) \tag{4}$$

$$A_{str2} = b_w (l_c \cos\theta_s + l_f \sin\theta_s) \tag{5}$$

$$A_{str3} = b_w (l_d \cos\theta_s + l_a \sin\theta_s) \tag{6}$$

$$A_{str4} = (A_{str1} + A_{str3}) / 2 \tag{7}$$

$$A_{str5} = (A_{str2} + A_{str3}) / 2 \tag{8}$$

Where l_a , l_b , and l_f are the widths of the support and load bearing plates (Fig. (1))

3. Derivation of Internal Forces and End Reactions

Assuming perfect elastic–plastic material properties for concrete and steel bars, the internal forces of the truss are solved. They are denoted as:

$$F_{c1} = A \cdot P \quad (9)$$

$$T_1 = B \cdot P \quad (10)$$

$$T_2 = C \cdot P \quad (11)$$

$$F_{c2} = D \cdot P \quad (12)$$

Where F_{c1} and F_{c2} represent the respective forces in the outer and interior concrete strut, T_1 and T_2 represent the respective tension forces in the top and bottom longitudinal reinforcement, and P represents the point load acting on the beam (Fig. (2)). The variables A , B , C , and D can be determined by means of the above mentioned parameters using the first principle analysis by applying virtual work method to the truss shown in Fig. (2). With releasing the intermediate support, the internal truss forces (F_o) will be calculated according to equilibrium equations as:

$$F_{oAB} = 0.5 \cot \theta_s \quad (13)$$

$$F_{oAC} = -0.5 / \sin \theta_s \quad (14)$$

$$F_{oBC} = 0.5 / \sin \theta_s \quad (15)$$

$$F_{oCC'} = -P \cot \theta_s \quad (16)$$

Applying vertical load of value 1.0 kN (downward) at the released support gives the internal forces (F_i) as:

$$F_{oAB} = P \cot \theta_s \quad (17)$$

$$F_{oAC} = -P / \sin \theta_s \quad (18)$$

$$F_{oBC} = \text{Zero} \quad (19)$$

$$F_{oCC'} = -\cot \theta_s \quad (20)$$

The cross-sectional areas of the lower and upper ties AB and CC' are A_{t1} and A_{t2} respectively with lengths l_e and young's modulus E_s . For compression struts AC and BC , the cross-sectional areas are respectively A_{str1} and A_{str2} with lengths $(l_e/2 \cos \theta_s)$ and young's modulus E_c . The vertical reaction at the intermediate support can be then calculated by applying the virtual work equations as follows:

$$\Sigma(F_i F_o \quad LE/A_i) = R_b \Sigma(F_i^2 LE/A_i) \quad (21)$$

The internal force in each member will be accordingly calculated according to the following equation:

$$F = F_o + R_b F_i \quad (22)$$

The variables A , B , C , and D can be determined by calculating the internal forces for each member and their values will be as follows:

$$A = (1/\sin \theta_s) [(g+m)/(f+2g+n+m)] \quad (23)$$

$$B = (\cot \theta_s) [(g+m)/(f+2g+n+m)] \quad (24)$$

$$C = (\cot \theta_s) [(0.5f+n/2-m/2)/(0.5f+g+n/2+m/2)] \quad (25)$$

$$D = (1/\sin \theta_s) [(f+g+n)/(f+2g+n+m)] \quad (26)$$

$$n = 0.5E_c / (A_{str4} \cos^3 \theta_s) \quad (27)$$

$$m = 0.5E_c / (A_{str5} \cos^3 \theta_s) \quad (28)$$

$$f = E_s / A_{t1} \quad (29)$$

$$g = E_s / A_{t2} \quad (30)$$

The reaction at outer support (R_o) and intermediate support (R_i) can be then calculated from Fig. (2) as:

$$R_o = F_{c1} \sin \theta_s \quad (31)$$

$$R_i = 2 F_{c2} \sin \theta_s \quad (32)$$

4. Evaluation of Compressive and Tensile Stresses for STM

The principal tensile stress f_t at the tension–compression nodal zone arises from the component force of longitudinal reinforcement in the direction perpendicular to the diagonal strut, namely, $T_s \sin \theta_s$. Thus, f_t can be expressed by:

$$f_t = k T_s \sin \theta_s / (A_c / \sin \theta_s) \quad (33)$$

Where $T_s \sin \theta_s / (A_c / \sin \theta_s)$ is the average equivalent tensile stress across the diagonal strut and A_c is the effective beam cross-sectional area, k in the numerator is a factor taking account of the non-uniformity of the stress distribution. A triangular stress distribution along the diagonal strut due to the presence of the bottom steel was assumed. According to force equilibrium, namely, by equating $T_s \sin \theta_s$ to the force represented by the triangular stress block. To satisfy both moment and force equilibrium, the stress distribution is shown in Fig. (4) and the factor k can be determined accordingly. First, consider one reinforcing bar that criss-crosses the diagonal strut and inclines at an angle θ_w from horizontal (Fig. (4)). The effect of single reinforcement T is “smeared” across the entire strut length. By applying the force equilibrium in the f_t direction to tensile force T of the steel bar and the idealized stress distribution along the diagonal strut (Fig. (4)), the following equations can be established:

$$[(k+k')/2] \rho_t \cdot b_w d_c / \sin \theta_s = T (\sin \theta_s + \sin \theta_w) \quad (34)$$

$$\rho_t = T (\sin \theta_s + \sin \theta_w) / (A_c / \sin \theta_s) \quad (35)$$

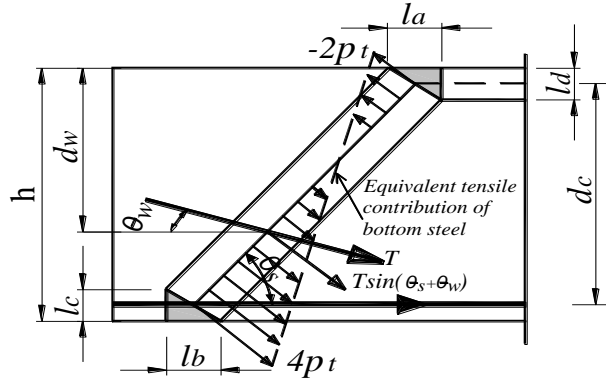


Figure (4) Determination of Tensile Stress Factors at Nodal Zones

Where k and k' are the stress distribution factors at the respective bottom & top nodal zones, θ_s is the diagonal strut angle, b_w is the beam width, and d_c is the beam effective depth taken as the vertical distance between the centroids of top and bottom nodal zones. From moment equilibrium about the top node between T and the idealized tensile stress distribution:

$$[k'/2 + (k-k')/3] (d_c/\sin\theta_s)^2 b_w \rho_t = T (\sin\theta_s + \sin\theta_w) \cdot (d_w/\sin\theta_s) \quad (36)$$

Comparing equations (34) and (36), the following factors for determining the principal tensile stress at the respective top and bottom nodal zones can be obtained:

$$k' = 4 - 6 (d_w/d_c) \quad (37)$$

$$k = 6 (d_w/d_c) - 2 \quad (38)$$

For the case of bottom reinforcement, (Fig. (4)), $d_w = d_c$ and $\theta_w = 0$, the stress distribution factor is:

$$k' = -2 \text{ (compression)} \quad (39)$$

$$k = 4 \text{ (tension)} \quad (40)$$

Thus, the principal tensile stress f_t in the model can be expressed as below:

$$f_t = 4 T_s \sin\theta_s / (A_c / \sin\theta_s) \quad (41)$$

The maximum tensile capacity in the f_t direction is a composite term and can be expressed by:

$$f_t = f_{st} + f_{tu} \quad (42)$$

The term f_{tu} represents the concrete tensile strength and is taken [3,4] as function of concrete compressive strength.

The term f_{st} represents the contribution from steel reinforcement. It consists of two parts: f_{sw} from the web reinforcement and f_{ss} from the longitudinal reinforcement.

$$f_{st} = f_{ss} + f_{sw} \quad (43)$$

The contribution of bottom longitudinal steel f_{ss} can be obtained in a similar fashion:

$$f_{ss} = 4 A_s f_y \sin\theta_s / (A_c / \sin\theta_s) \quad (44)$$

The presence of web reinforcement in the strut restricts the diagonal crack from quickly propagating to either end of the strut. The tensile contribution of web reinforcement at the interface of the nodal zone can be calculated as:

$$f_{sw} = A_{sw} f_{yw} \sin(\theta_s + \theta_w) / (A_c / \sin\theta_s) \quad (45)$$

Where $A_{sw} = n_s A_{swl}$ represents the total area of web reinforcement criss-crossing the concrete strut, and A_{swl} is the area of an individual web steel. For the common cases of vertical ($\theta_w = 90^\circ$) or horizontal ($\theta_w = 0^\circ$) web reinforcement, Equation (45) reduces to:

$$f_{sv} = A_{sv} f_{yv} \sin 2\theta_s / 2A_c \quad (46)$$

$$f_{sh} = A_{sh} f_{yh} \sin^2\theta_s / A_c \quad (47)$$

where, A_{sv} and A_{sh} are the respective total areas of vertical and horizontal web steel within the shear span.

The principal compressive stress f_2 in the direction of the left diagonal strut at the bottom nodal zone is computed from:

$$f_2 = (F_c - T \cos\theta_s) / A_{str} \quad (48)$$

Where, A_{str} is the cross-sectional area at the bottom end of the diagonal strut. The component force $T \cos\theta_s$ of the main longitudinal reinforcement is omitted for simplicity and conservatism.

The softening effects exists in concrete under a state of biaxial tension-compression, that is, the presence of the transverse tensile strain leads to a deterioration of the compressive strength. In general, the equation that yields the concrete softening coefficient ν can be expressed as:

$$F_c / A_{str} = \nu f_{cu} \quad (48)$$

The modified Mohr-Coulomb criterion is adapted for considering concrete softening effect.

$$(f_1/f_t) + (f_2/f_{cu}) = 1 \quad (49)$$

Where f_1 and f_2 are principal tensile and compressive stresses at the nodal zone respectively, f_{cu} is the compressive strength of cube, representing the maximum compressive strength in the f_2 direction; f_t represents the maximum tensile capacity in the f_1 direction.

5. Derivation of Shear Carrying Capacity for Proposed STM

Three tension–compression nodal zones are identified in the STM for deep beams as shown in Fig. (1). Morh's failure criterion is applied to the three nodal zones, as follows:

- At nodal zone (A), the principal tensile stress f_{1A} across the diagonal strut and the principal compressive stress f_{2A} in the diagonal strut can be obtained as follows:

$$f_{1A} = 4T_2 \sin\theta_s / (A_c / \sin\theta_s) = 4C \sin^2\theta_s \cdot (P/A_c) \quad (50)$$

$$f_{2A} = (F_{c1} - T_2 \cos\theta_s) / A_{str1} = (A - C \cos\theta_s) \cdot (P/A_{str1}) \quad (51)$$

From (49), (50) and (51), the following expression can be derived for the ultimate force P_{nA} :

$$P_{nA} = 1/[4C \sin^2\theta_s / (f_{1A} A_c) + (A - C \cos\theta_s) / (f_{cu} A_{str1})] \quad (52)$$

Where f_{1A} is the maximum tensile capacity of nodal zone A in f_l direction and can be similarly expressed by:

$$f_{1A} = 4A_{s2} f_y \sin\theta_s / (A_c / \sin\theta_s) + A_{sw} f_{yw} \sin(\theta_s + \theta_w) / (A_c / \sin\theta_s) + f_{tu} \quad (53)$$

- At nodal zone (B), the principal tensile stress f_{1B} across the diagonal strut at nodal zone B consists of two components: the contributions from the top and bottom reinforcement. As the factor k is -2 (compression) for top steel and 4 (tension) for bottom steel, the combined f_{1B} can be expressed as below:

$$f_{1B} = (4T_2 \sin\theta_s - 2T_1 \sin\theta_s) / (A_c / \sin\theta_s) = (4C - 2B) \sin^2\theta_s \cdot (P/A_c) \quad (54)$$

The principal compressive stress at nodal zone B is obtained similarly as nodal zone A:

$$f_{2B} = (F_{c2} - T_2 \cos\theta_s) / A_{str2} = (D - C \cos\theta_s) \cdot (P/A_{str2}) \quad (55)$$

From Equations (54), (59) and (60), the following expression can be derived for the ultimate load P_{nB} :

$$P_{nB} = 1/[(4C - 2B) \sin^2\theta_s / (f_{1B} A_c) + (D - C \cos\theta_s) / (f_{cu} A_{str2})] \quad (56)$$

It is noteworthy that the maximum tensile capacity of nodal zone B (f_{1B}) is expressed by:

$$f_{1B} = (4T_{2max} - 2T_{1a}) / (A_c / \sin^2\theta_s) + A_{sw} f_{yw} \sin(\theta_s + \theta_w) / (A_c / \sin\theta_s) + f_{tu} \quad (57)$$

$$T_{1a} = \text{Min} \{T_{1max}, (B/C) T_{2max}\} \quad (58)$$

Where T_{2max} is the yield strength of bottom steel and T_{1a} is the corresponding tension force in the top steel at the yielding of bottom steel. The term T_{1a} should not exceed the yield strength of top steel.

- At nodal zone (C), similarly:

$$f_{1C} = (4T_1 \sin\theta_s - 2T_2 \sin\theta_s) / (A_c / \sin\theta_s) = (4B - 2C) \sin^2\theta_s \cdot (P/A_c) \quad (59)$$

$$f_{2C} = (F_{c2} - T_1 \cos\theta_s) / A_{str3} = (D - B \cos\theta_s) \cdot (P/A_{str3}) \quad (60)$$

From Equations (49), (59) and (60), the following expression can be derived for the ultimate load P_{nC} :

$$P_{nC} = 1/[(4B - 2C) \sin^2\theta_s / (f_{1C} A_c) + (D - B \cos\theta_s) / (f_{cu} A_{str3})] \quad (61)$$

The term f_{1C} in Equation (61) is the maximum tensile capacity of nodal zone C:

$$f_{1C} = (4T_{1max} - 2T_{2a}) / (A_c / \sin^2\theta_s) + A_{sw} f_{yw} \sin(\theta_s + \theta_w) / (A_c / \sin\theta_s) + f_{tu} \quad (62)$$

$$T_{2a} = \text{Min} \{T_{2max}, (C/B) T_{1max}\} \quad (63)$$

Similarly, T_{1max} is the yield strength of top steel and T_{2a} is the corresponding tension force in the bottom steel at the yielding of top steel. T_{2a} should not exceed the yield strength of bottom steel.

Thus the predicted ultimate load P will be the minimum among Equations (52), (56) and (61), denoted as P_n .

$$P_n = \text{Min} (P_{nA}, P_{nB}, P_{nC}) \quad (64)$$

6. Validation and Comparative Studies

Sixty continuous RC deep beams reported by many researchers [1,2,5-10] have been evaluated by the proposed model [1]. The details of the specimens and the predicted-versus-actual ultimate strength ratios are summarized in [1]. The tested beams had an overall depth ranging from 400 to 1000 mm, and an (a/d) ratio from 0.5 to 2.25. The top-and-bottom longitudinal main reinforcement ratios ranged from 0.07% to 1.88% and 0.32% to 1.88%, respectively. The vertical and horizontal web reinforcement ratios ranged from zero to 0.90% and zero to 1.71%, respectively. The concrete cube strengths ranged from 25 MPa to 60 MPa. The predicted ultimate strength (P_n) versus the obtained experimental strength (P_{exp}) is plotted in Fig. (5). It shows the comparison of model predictions with 60 test results. Generally speaking, the proposed model is on the safe side and gives consistent predictions. In Figure (5), the obtained experimental strength (P_{exp}) and the predicted strength (P_n) are listed. The overall average value of the ratio between the experimental strength to the predicted strength is of value 1.09 and a standard deviation of 0.12. These values indicate that the proposed STM gives good predictions with consistent results.

For the 60 specimens, the predicted ultimate strengths for the STM by the ECP code [3] (P_{ECP}) and the ACI code [4] (P_{ACI}) were calculated. The predicted ultimate strengths by the ECP code (P_{ECP}) and the ACI code (P_{ACI}) versus the obtained experimental strength (P_{exp}) are plotted in Figures (6) and (7) respectively. The overall average ratio between experimental strength (P_{exp}) and predicted strength is 1.20 and 1.16 with standard deviations of 0.17 and 0.15 for ECP and ACI design codes, respectively. These values indicate that the STM of the ECP code [3] and the ACI code [4] underestimate the strength of continuous RC deep beams. Conservatively, the STM of the ECP design code predicts the strength on the safe side. Generally, the predictions of the STM of the ACI design codes are on the safe side with conservative values.

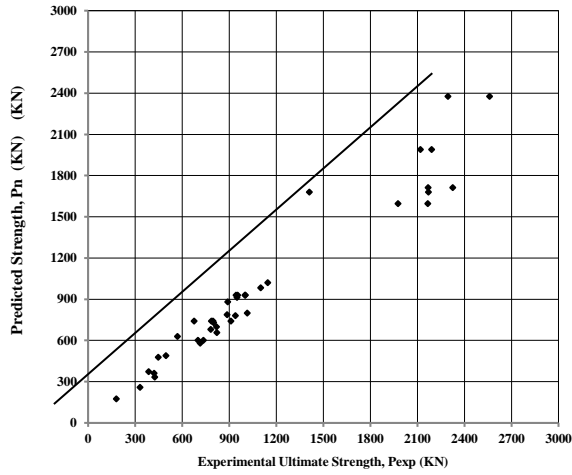


Figure (5) Ultimate Strength Predictions by the Proposed STM for Deep Beams

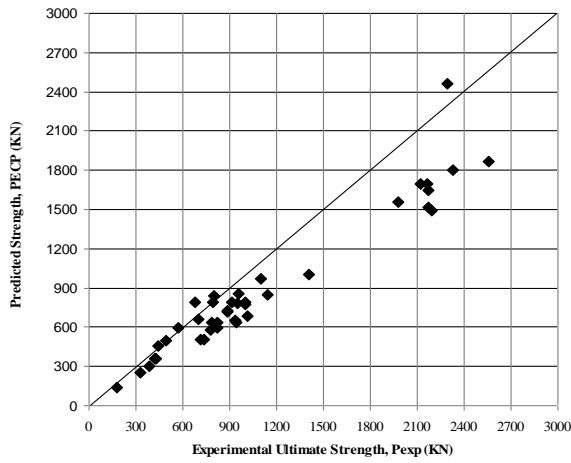


Figure (6) Ultimate Strength Predictions by the STM of ECP Design Code for Deep Beams

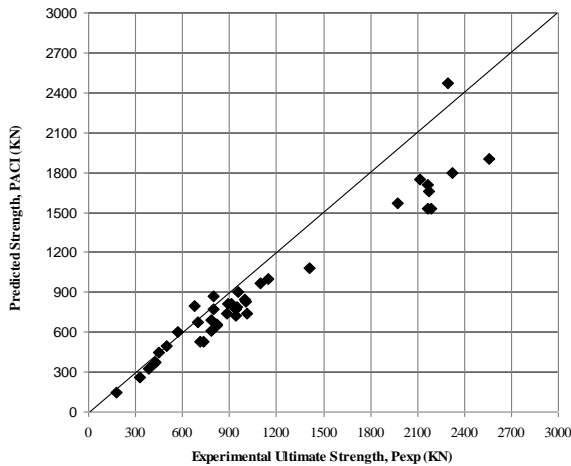


Figure (7) Ultimate Strength Predictions by the STM of ACI Design Code for Deep Beams

The predicted reaction at the internal support by the proposed STM (R_{ith}) versus the obtained experimental reaction (R_{iex}) is plotted in Fig. (8) for 60 specimens. Generally, the proposed STM predicts well the reaction at the internal support compared to the experimental results. The overall average value of the ratio between the experimental reaction (R_{iex}) to the predicted reaction (R_{ith}) is of value 1.04 and a standard deviation of 0.14.

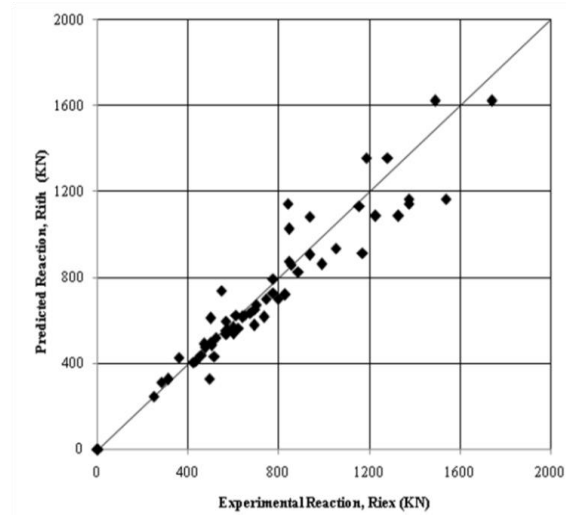


Figure (8) Predictions for Internal Support Reactions by the Proposed STM

7. Conclusions

The following points are drawn from the validation and comparative studies of the proposed STM:

1- Comparison of the predictions of the proposed (STM) with 60 test results indicates that the model generally performs well in predicting the ultimate load carrying capacities for continuous deep beams. The proposed STM is on the safe side and gives consistent predictions. The overall average value of the ratio between the experimental strength to the predicted strength is of value 1.09 and a standard deviation of 0.12.

2- The predictions of STM of the ECP code [3] and the ACI code [4] underestimate the strength of continuous RC deep beams. The overall average ratios between experimental strength and predicted strength are respectively 1.2 and 1.16 for ECP and ACI design codes. The corresponding standard deviations are 0.17 and 0.15 respectively.

3- The proposed STM predicts well the reaction at the internal support compared to the experimental results. The predictions are consistent and accurate for continuous deep beams with different geometrical properties, concrete compressive strengths and total reinforcement ratios. The overall average value of the ratio between the experimental reaction to the predicted reaction is of a value 1.04 and a standard deviation of 0.14.

REFERENCES

- [1] T.S. Mustafa, *Behavior of Reinforced Concrete Continuous Deep Beams*, Ph.D. Thesis, Faculty of Engineering at Shoubra, Benha University, Egypt, 2012.
- [2] N. Zhang, K. H. Tan, *Direct Strut-and-Tie Model for Single Span and Continuous Deep Beams*, *Engineering Structures*, V. 29, No. 11, 2007, pp. 2987-3001.
- [3] Egyptian Code of Practice ECP 203, *Design and Construction of Reinforced Concrete Structures*, Ministry of Building and Construction, 2010.
- [4] ACI Committee 318, *Building Code Requirements for Structural Concrete (ACI 318-08) and Commentary (ACI 318-R-08)*, ACI, Farmington Hills, 2008.
- [5] D. M. Rogowsky, J. M. MacGregor, and S. Y. Ong, *Tests of Reinforced Concrete Deep Beams*, *ACI Journal*, V. 83, No. 4, July-Aug. 1986, pp. 614-623.
- [6] A. Adly, *Behavior of Bottom-Loaded Continuous Deep Beams*, PhD Thesis, Faculty of Engineering, Cairo University, Egypt, 1999
- [7] A. F. Ashour, *Tests of Reinforced Concrete Continuous Deep Beams*, *ACI Structural Journal*, V. 94, No.1, Jan.-Feb. 1997, pp. 3-12.
- [8] J. C. Walraven, *The Behavior of Reinforced Concrete Continuous Deep Beams*, PhD Thesis, Delft University Press, Netherlands, Jan. 2000.
- [9] El-Zoughiby, M.E., El-Metwally, S.E., Al-Shora, A.T. and Agieb, E.E., *Strength Prediction of Continuous R/C Deep Beams Using the Strut-and-Tie Method*, *Arab J. Sci. Eng. AJSE.*, Published on line September 2013. DOI: 10.1007/s13369-013-0755-2
- [10] Panjehpour, M, Chai, H. K and Voo, Yen Lei, *Refinement of Strut-and-Tie Model for Reinforced Concrete Deep Beams*, Jose Manuel Garcia Aznar, Academic Editor, Published online June 2015. PLoS One 10(6): e0130734. DOI: 10.1371/journal.pone.0130734.